ELSEVIER

Journal of Structural Geology 29 (2007) 983–1001

JOURNAL OF STRUCTURAL GEOLOGY

www.elsevier.com/locate/jsg

Testing the utility of the porphyroclast hyperbolic distribution method of kinematic vorticity analysis

Adam M. Forte*, Christopher M. Bailey

Department of Geology, College of William and Mary, P. O. Box 8795, Williamsburg, VA 23187, USA

Received 13 July 2006; received in revised form 8 January 2007; accepted 30 January 2007
Available online 8 February 2007

Abstract

Kinematic vorticity (W_k) is a dimensionless measure of rotation relative to finite stretching and is essential for complete understanding of flow in ductile shear zones. The porphyroclast hyperbolic distribution (PHD) method is a widely used technique for estimating W_k based on the acute angle between the flow eigenvectors determined from the orientations of back-rotated σ porphyroclasts. The utility of the PHD was tested with Tertiary ultramylonites from the Santa Catalina Mountains, Arizona, Proterozoic ultramylonites from the Virgin Mountains, Nevada, and a Paleozoic ultramylonite from the Hylas zone in the Virginia Piedmont.

Bootstrapping statistics and a computational sieving process were used to analyze the PHD data set. Average standard deviations of the bootstrapped data sets yield a 1σ standard error of $\pm 9\%$ for a W_k-value measured as a % simple shear. Sieving results imply that back-rotated porphyroclasts may not orient parallel to the extensional eigenvector. The PHD method is useful for discerning between deformations that are pure shear dominated, general shear, or simple shear dominated, but is not accurate enough to report precise W_k-values. When performed on multiple sections the PHD method can identify zones of monoclinic versus triclinic shear.

Keywords: Porphyroclast hyperbolic distribution method; Kinematic vorticity analysis; Triclinic deformation; Ultramylonite; Bootstrapping

1. Introduction

Ductile shear zones are common deformational features in many tectonic settings and accommodate significant amounts of strain across major crustal boundaries. To understand the flow histories of these zones, quantitative knowledge of shear zone kinematics is necessary. Kinematic vorticity and three-dimensional strain symmetry are needed to accurately describe the transport direction, amount of displacement, and shortening across a shear zone. Despite their importance, both quantities are commonly overlooked in many kinematic analyses and tectonic reconstructions.

Kinematic vorticity (W_k) is a dimensionless measure of rotation relative to strain and characterizes the amount of shortening proportional to displacement. W_k was originally defined as an instantaneous rotation relative to the instantaneous stretching at a point (Truesdell, 1953; Means et al., 1980). In most settings structural geologists observe the end product of flow and cannot measure instantaneous quantities. Tikoff and Fossen (1995) transformed W_k to represent three-dimensional finite deformation parameters, defined in terms of shear strains and stretches. Other studies have used W_n (neutral vorticity number, Passchier, 1988) and W_m (mean vorticity number, Passchier, 1988) to define vorticity. For cases of simple shear and sub-simple shear, W_k is measured on a scale between 0 and 1, with 0 being pure shear and 1 being simple shear. The W_k scale is not linear, but can be converted to a linear scale by considering the percent of a deformation resultant from simple shear (Fig. 1). Although other workers have categorized deformations as either pure- or simple shear dominated, in reality

* Corresponding author. Present address: Department of Geology, University of California, Davis, CA 95616, USA. Tel.: +1 530 754 8452; fax: +1 530 752 0951.
E-mail address: forte@geology.ucdavis.edu (A.M. Forte).

0191-8141/$ - see front matter © 2007 Elsevier Ltd. All rights reserved.
doi:10.1016/j.jsg.2007.01.006

there is a continuum from pure shear to simple shear. We propose three separate fields for pure, general, and simple shear dominated deformations (Fig. 1) (see also Bailey et al., 2007). Pure shear dominated deformations have W_k-values of 0–0.3, corresponding to less than 20% simple shear. In contrast, simple shear dominated deformations have W_k-values of greater than 0.95, corresponding to greater than 80% simple shear. General shear occupies the range between 0.3 and 0.95 (Fig. 1). While the exact placement of the boundaries is open to interpretation, dividing this continuum into three fields serves to highlight the differences in the resultant deformations (Fig. 2; Bailey et al., 2007). In essence, simple shearing produces displacement with little shortening/thinning, general shear is a combination of both thinning and displacement, and pure shear zones experience a great deal of thinning with modest displacement relative to overall strain.

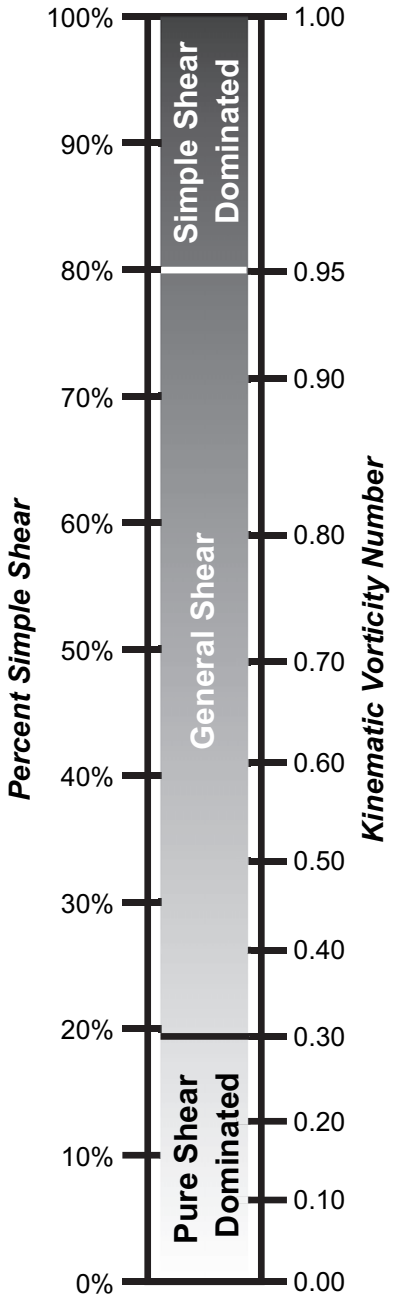

Fig. 1. Scale relations between the W_k-value and percent simple shear. Zones of pure shear dominated, general shear, and simple shear dominated deformations as used in this paper are illustrated.

The symmetry of a finite deformation is defined by the geometry of the rotation axis of the finite deformation with respect to the principal strain axes and can be orthorhombic, monoclinic, or triclinic (Jiang and Williams, 1998; Lin et al., 1998; Passchier, 1998). Strain symmetry depends upon the orientations of the shear direction with respect to the principal stretching directions of the shear zone (Robin and Cruden, 1994; Jiang and Williams, 1998). Orthorhombic deformation symmetries are characterized by a parallelism between the finite strain elements (foliation and lineation) and the high-strain zone boundary and an abundance of symmetric structures. Monoclinic deformation produces an angular discordance between the foliation and shear zone boundaries as well as asymmetric structures normal to the foliation and parallel to the elongation lineation. Triclinic deformation is characterized by asymmetric structures on sections both normal and parallel to elongation lineations (Jiang and Williams, 1998; Lin et al., 1998; Bailey et al., 2002). In zones of heterogeneous triclinic deformation, elongation lineations may vary between strike-parallel and dip-parallel orientations (Lin et al., 1998; Lin and Jiang, 2001).

Traditionally, shear zones were assumed to be either the product of pure or simple shear and have an orthorhombic or monoclinic strain symmetry (Fig. 2). However, zones of general shear are common in many different tectonic settings (Wallis et al., 1993; Simpson and De Paor, 1993, 1997; Tikoff and Fossen, 1995; Jezek et al., 1996; Jiang and Williams, 1998; Bailey and Eyster, 2003; Bailey et al., 2004). General shear zones accommodate thinning or widening in addition to the simple shear component and therefore can record less displacement than a simple shear zone given similar amounts of strain (Fig. 2). Modeling and field observations indicate that monoclinic shear zones are not as ubiquitous as once thought, and triclinic shear zones exist (Robin and Cruden, 1994; Lin et al., 1998; Passchier, 1998; Bailey et al., 2002). In monoclinic shear zones the transport direction, the projection of the maximum elongation direction onto the flow plane, is either parallel to the mylonitic lineation or if the zone is transpressional (Sanderson and Marchini, 1984) at a right angle to the lineation, but if the zone is triclinic then the transport direction has no set orientation with respect to lineation (Jiang and Williams, 1998; Lin et al., 1998; Fig. 3).

Various techniques have been proposed to measure the kinematic vorticity number in naturally deformed rocks and these include methods that measure the finite rotation of spherical objects with respect to the instantaneous stretching axes, the distribution of shortened and extended lines, asymmetry of stair-stepping objects, the nature of blocked objects, the geometry of crystallographic fabrics and the R_s-Θ method (Ghosh, 1987; Passchier, 1988; Vissers, 1987; Wallis, 1992, 1995; Fossen & Tikoff, 1993; Bailey and Eyster, 2003; Law et al., 2004). Many of these methods either require specific

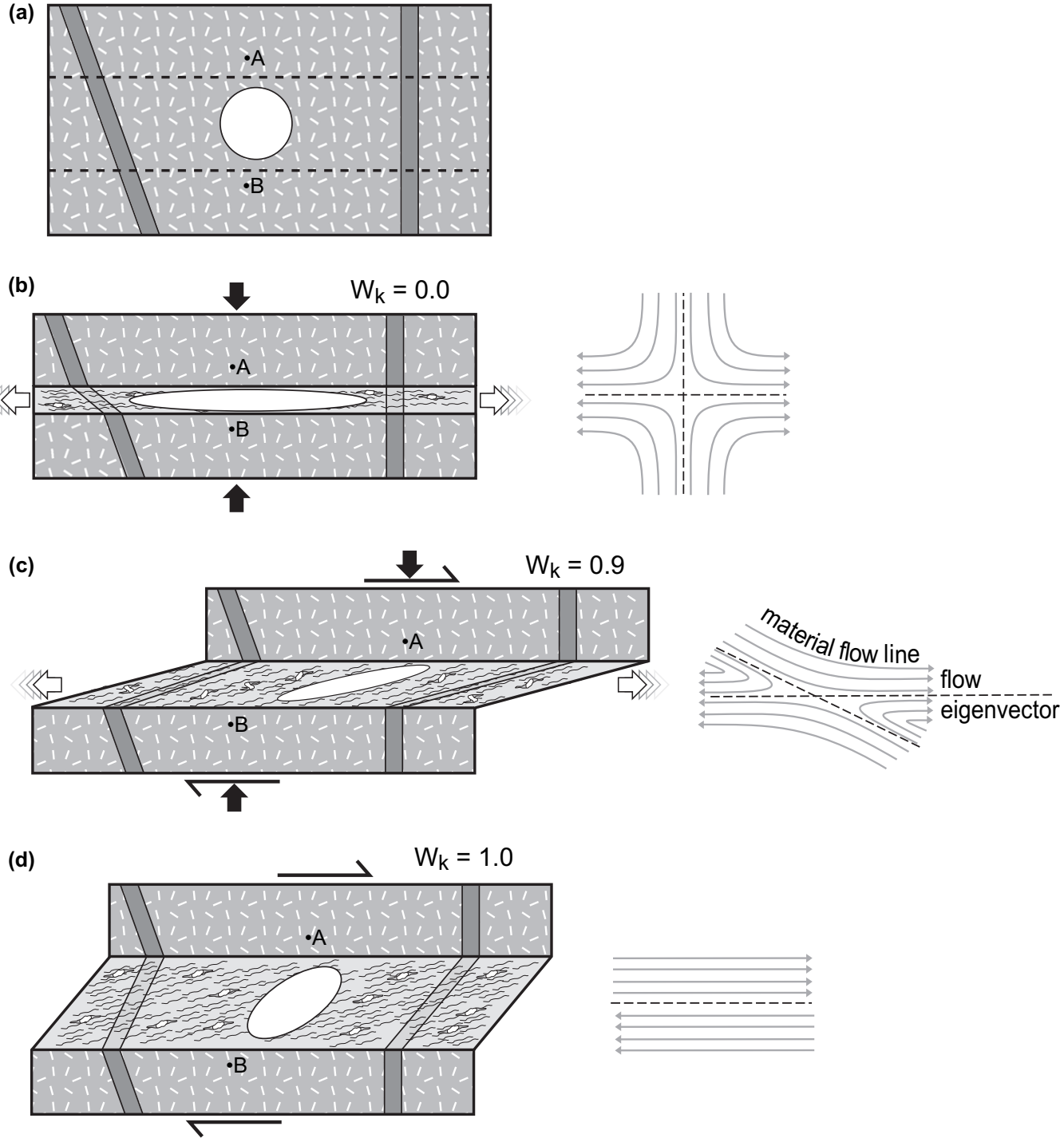

Fig. 2. (a) The initial condition before high-strain zone formation. Dikes, points A and B, and the strain ellipse are provided as reference. (b) Pure shear deformation with two eigenvectors orthogonal to each other. White arrows indicate zone parallel stretching. (c) General shear deformation with a W_k-value of 0.9. The acute angle between the two eigenvectors is correspondingly 26°. (d) Simple shear deformation with one eigenvector.

criteria that must be met in order for them to be effective or in practice are not accurate kinematic vorticity gauges. Strain symmetry affects the kinematic vorticity in predictable ways, so a reliable method of measuring kinematic vorticity should also provide information on the strain symmetry of a given deformation (Fig. 3). The porphyroclast hyperbolic distribution (PHD) method of Simpson and De Paor (1997) is a method for measuring kinematic vorticity in high-strain ductily deformed rocks. Here we investigate the accuracy of the PHD method as a kinematic vorticity gauge and explore the ability of the method to evaluate three-dimensional strain symmetry.

2. Instantaneous flow and strain symmetry

Understanding instantaneous flow quantities during deformation provide the basis for many kinematic methods, including

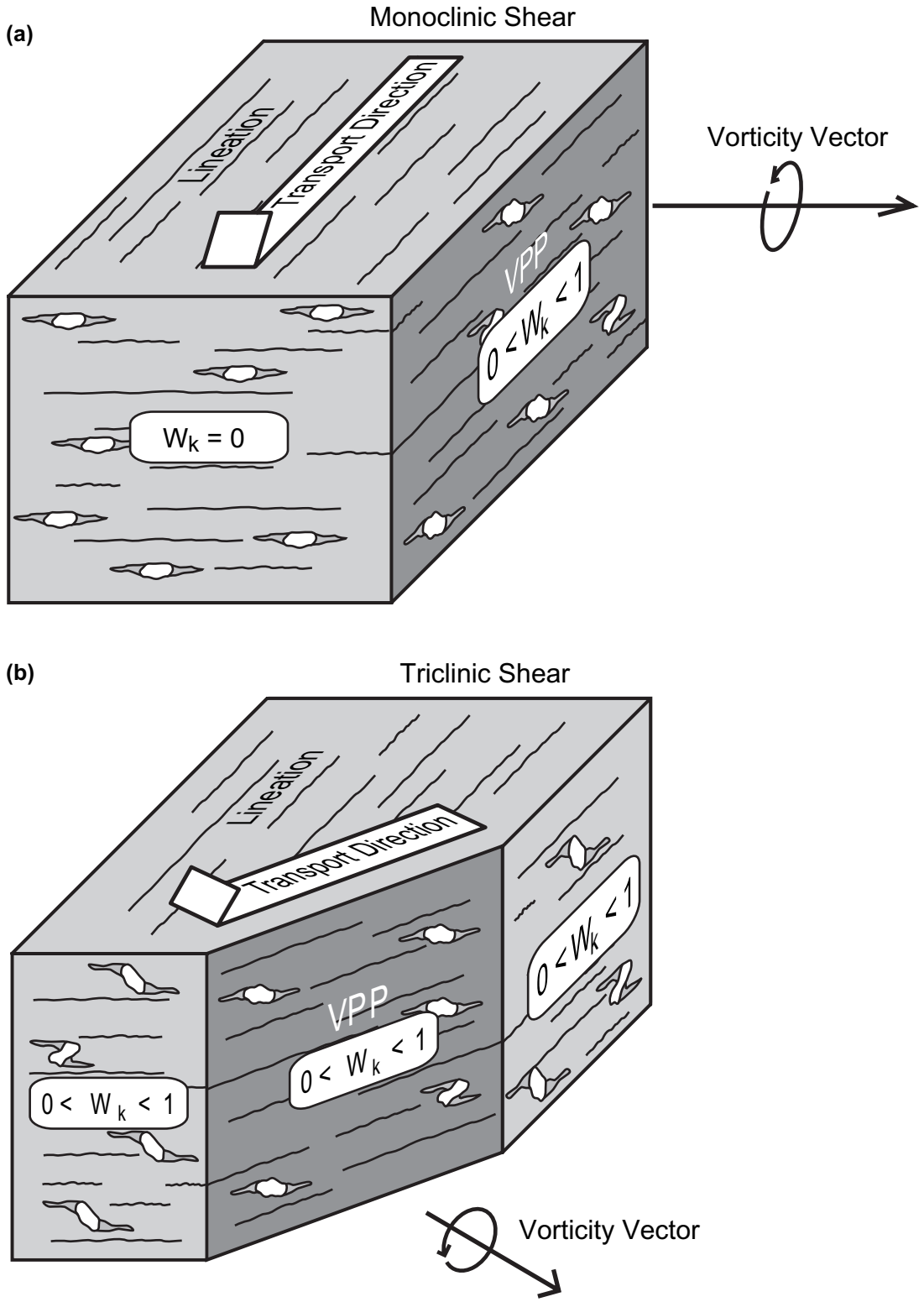

Fig. 3. (a) Block diagram of monoclinic shear. The transport direction and correspondingly the vorticity profile plane (VPP) are parallel to the lineation. Maximum symmetry is expected in the lineation-normal plane with a zero W_k-value. (b) In triclinic shear, the VPP and transport direction are not parallel to the lineation. Therefore, both lineation-parallel and normal planes should have non-zero W_k-values, but neither are the VPP.

the porphyroclast hyperbolic distribution method. Instantaneous stretching axes (ISA) are three principal directions of stretching present in a deforming fluid and correspond to three directions of maximum, intermediate, and minimum stretch within a flow field (Passchier, 1988, 1997). Flow eigenvectors (flow apophyses of Passchier, 1988) are axes defining directions in which material lines only shorten and lengthen, but do not rotate. In orthorhombic coaxial flows, or pure shear, the two flow

eigenvectors are orthogonal and parallel to the ISA (Fig. 2) (Simpson and De Paor, 1993). Simpson and De Paor (1993) divide non-coaxial flow into two subcategories, simple shear and general shear. The two eigenvectors are parallel to each other and the flow plane during simple shear. General shear is characterized by two eigenvectors, with one eigenvector parallel to the flow plane and the other eigenvector inclined at an acute angle to the flow plane (Simpson and De Paor, 1993). In general shear, the eigenvector oblique to the flow plane is commonly referred to as the unstable eigenvector (Fig. 2) (Simpson and De Paor, 1993; Piazolo et al., 2002).

The behavior of porphyroclasts entrained within the flow depends on the flow type (i.e. orientation of the eigenvectors) and the axial ratio of the porphyroclast in question (Ghosh and Ramberg, 1976; Passchier, 1987, 1997; Simpson and De Paor, 1993, 1997; Piazolo et al., 2002; Giorgis and Tikoff, 2004). During deformation, rigid porphyroclasts with an aspect ratio greater than a critical value rotate towards material attractors nearly coincident with the flow eigenvectors (Simpson and De Paor, 1993, 1997; Passchier, 1997). Porphyroclasts with axial ratios smaller than this critical value rotate independent of the bulk flow attractors (Passchier, 1987; Mulchrone et al., 2005).

In the case of general shear, porphyroclasts can either rotate backwards or forwards towards the flow attractors (Passchier, 1987; Simpson and De Paor, 1993, 1997). Porphyroclasts that forward rotate reach a stable end position within the obtuse angle field between the two eigenvectors (Ghosh and Ramberg, 1976). Simpson and De Paor (1993) hypothesized that backward rotated porphyroclasts would rotate to an instantaneous stable position where forward rotation of the simple shear component was counteracted by backward rotation from the pure shear component. Later, Simpson and De Paor (1997) indicated that the stable position reached by the contributions of the pure and simple shear components would define the unstable eigenvector in agreement with Piazolo et al. (2002). Porphyroclasts that have reached a stable end position, through forward or backward rotation, can be identified by sigma tails (Passchier, 1987). Sigma tails are hypothesized to form during slow rotations of porphyroclasts, which occurs as they approach their stable end positions. Backward rotated porphyroclasts are identified by long axes orientations antithetic to the overall sense of shear and the presence of synthetic sigma tails on antithetic porphyroclasts. Synthetic sigma tails on antithetically oriented porphyroclasts must be produced through back rotation of the porphyroclast, because forward rotation of an antithetic porphyroclast would inhibit tail formation (Fig. 4). Porphyroclasts will only reach stable end positions if sufficient amounts of strain have accumulated.

Finite strain symmetry is independent of the type of flow. Monoclinic strain symmetry produces a vorticity vector parallel to one of the ISA of the flow (Passchier, 1998). This assumption implies that the vorticity vector is within foliation and is either parallel or normal to the lineation (Fig. 3). The vorticity vector is referenced relative to the plane orthogonal to the vector (Passchier, 1998). Maximum rotation within the flow occurs within this vorticity profile plane (VPP) and the plane is considered to contain the shear direction (Robin and Cruden, 1994). Relations between the VPP, lineation, and foliation depend upon the geometry of the shear zone (Fig. 5; Passchier, 1998). General shear zones should have maximum asymmetry in the VPP. In monoclinic general shear zones, the maximum asymmetry plane (and VPP) should be the lineation-parallel foliation-normal plane. Furthermore, the plane normal to both foliation and lineation is expected to have maximum symmetry, because material will not rotate in this plane and will record only the pure shear component of the general shear deformation (Fig. 3).

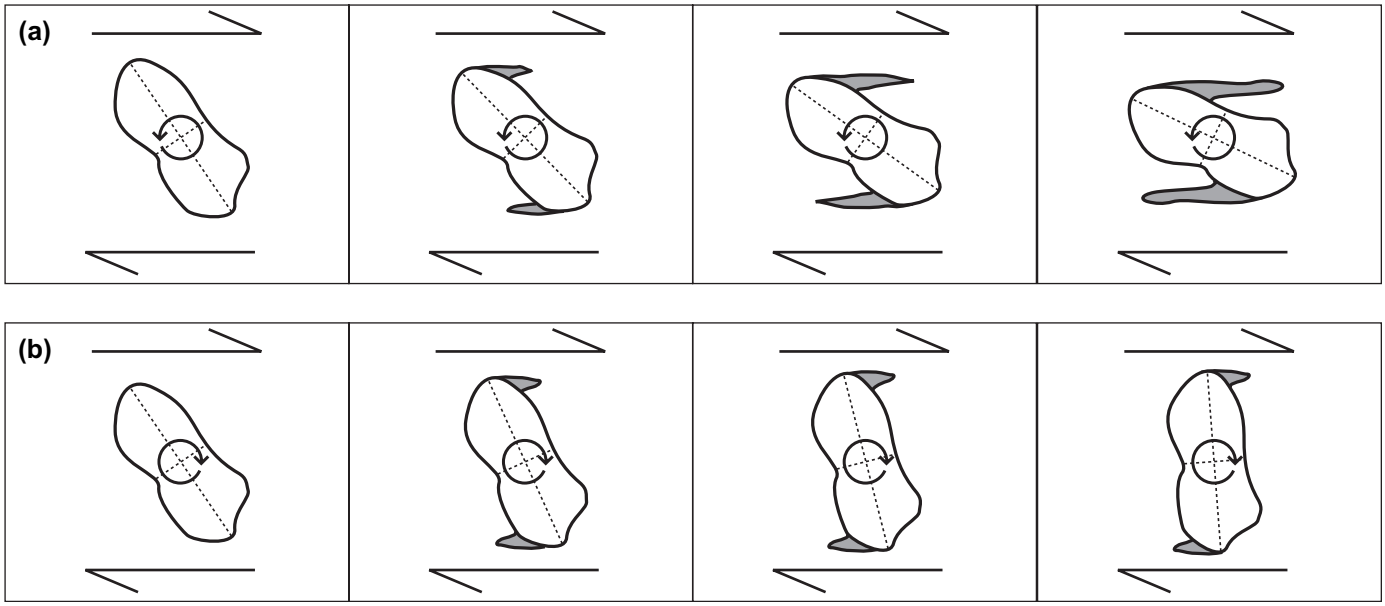

Fig. 4. Tail formation on rotating porphyroclasts. (a) Sigma tails growing on a back-rotating porphyroclast. (b) Growth of sigma tails is inhibited by forward rotation of a porphyroclast with a long axis oriented antithetic to the sense of shear. Presence of sigma tails on antithetically oriented porphyroclasts is evidence of back rotation.

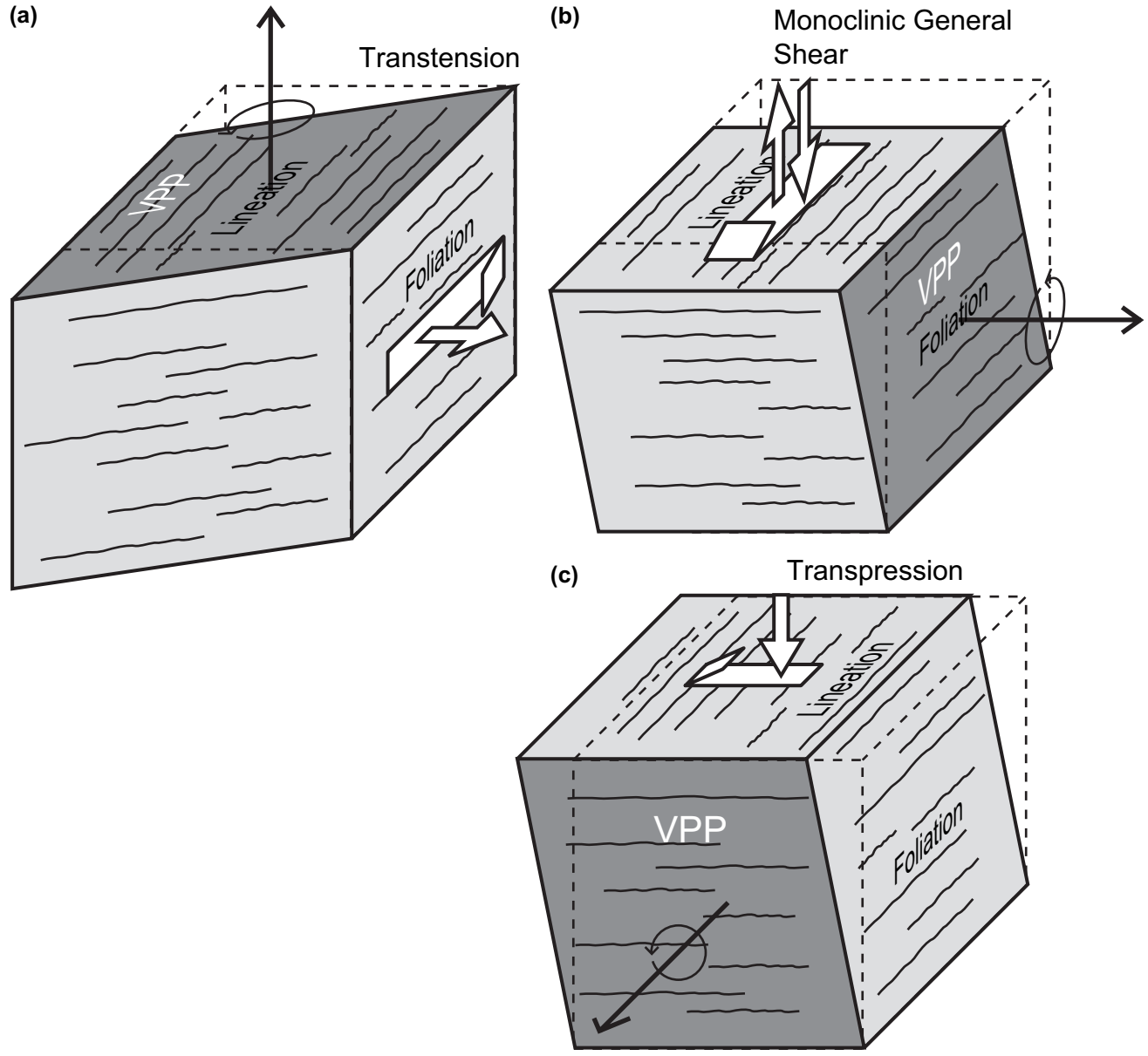

Fig. 5. Relations between the location of the VPP, lineation, and foliation in monoclinic shear zones as defined by Passchier (1998). Dotted lines are an aid to the visualization of the three-dimensional shapes of the figures. White arrows indicated shear directions and directions of shortening and extension. (a) Transtension, the VPP is parallel to both foliation and lineation; the zone widens with increasing deformation. (b) Monoclinic general shear, the VPP is parallel to lineation and orthogonal to foliation; the zone can widen or shorten. (c) Transpression, the VPP is orthogonal to both lineation and foliation; the zone shortens with increasing deformation.

If both the shear direction and vorticity vector make an angle with the ISA, then the flow is triclinic (Jiang and Williams, 1998). Triclinic shear is analogous to multiple instantaneous monoclinic deformations superimposed on the previous deformation, but between each incremental monoclinic deformation, the shear direction is changed, and the end result yields a single triclinic deformation. In triclinic shear zones, the lineation is not expected to be parallel to the shear direction, but rather oriented between the ISA and the finite strain axes (Jiang and Williams, 1998). Orientations of lineations would also be expected to change with respect to the vorticity vector throughout the shear zone (Robin and Cruden, 1994; Lin et al., 1998; Lin and Jiang, 2001). For a triclinic deformation the VPP is no longer parallel to fabric elements in the rock (Fig. 3). In the field, the identification of triclinic deformation has relied on the presence of a wide variation of lineation orientations within a shear zone and a noticeable porphyroclast asymmetry in both lineation-normal and lineation-parallel planes.

3. The porphyroclast hyperbolic distribution method

Simpson and De Paor (1993, 1997) proposed the porphyroclast hyperbolic distribution (PHD) method for measuring the kinematic vorticity number that is based on the premise that the orientation of the long axes of backward rotated grains within the acute angle field between the flow eigenvectors

delineates the orientation of the unstable eigenvector. The stable eigenvector is assumed to be parallel with foliation (Simpson and De Paor, 1997). Porphyroclasts in a given plane of a sample are identified as either forward or backward (Fig. 4) rotated based on the orientation of long axes relative to the overall sense of shear (e.g. Simpson and De Paor, 1993, 1997). The angle between the long axis of the grain and the normal to foliation is the phi (ϕ) angle, with positive ϕ values indicating forward rotated grains and negative ϕ values indicating back-rotated grains. Axial ratios (R) of the porphyroclasts are also measured. Both the ϕ and R-values are plotted on a hyperbolic stereonet (De Paor, 1988). A hyperbola is drawn to include all of the back-rotated grains, and the angle between the two limbs of the hyperbola represents the acute angle between the two eigenvectors, such that the cosine of this angle (ν) yields the kinematic vorticity number (Bobyarchick, 1986):

$$W_k = \cos(\nu). \quad (1)$$

4. Methods

4.1. The modified PHD method

We analyzed ultramylonites because they are the product of high-strain flows with clearly defined porphyroclasts that are likely to have reached a stable final position (if particular porphyroclasts are able to stabilize within a flow). In their original discussion of the PHD method, Simpson and De Paor (1997) advised that the analysis be done on lineation-parallel, foliation-normal planes because this is assumed to be the vorticity profile plane for monoclinic deformations. This does not imply that the method is unsuitable or inaccurate for analyzing planes in other orientations, but rather that for monoclinic deformations, other planes would not yield kinematic vorticities characteristic of the bulk flow (Fig. 3). If the sample was instead a product of a triclinic deformation, then kinematic vorticity analysis of non-lineation-parallel, foliation-normal planes should yield non-zero W_k-values (Fig. 3).

The presence of synthetic sigma tails on antithetically oriented porphyroclasts was used as a proxy for back rotation throughout the thin section in question. For each sample, three thin sections from both the lineation-parallel and lineation-normal planes were analyzed (all planes discussed here, and subsequently, are normal to foliation). Two samples that were sufficiently large were analyzed on planes at 30° and 60° from the lineation-parallel plane. More than 40 of the largest back-rotated porphyroclasts were measured in each thin section; with grains being traced by hand from micrographic images and then analyzed digitally. Plotting the data on a hyperbolic net is not necessary because the porphyroclast with the lowest ϕ angle always defined the kinematic vorticity number. The kinematic vorticity value is thus given by:

$$W_k = \cos(90 - \phi) \quad (2)$$

where the ϕ is the smallest angle made with the normal to foliation by back-rotated grains. Grain orientations are more easily visualized with a radial distribution plot than a hyperbolic net (Fig. 6). Porphyroclasts with small axial ratios (less than 1.4) were removed from consideration because sub-spherical grains are not actually back-rotated, but rather are continuously forward rotated and hence will give a false reading of kinematic vorticity (Passchier, 1987). Although an axial ratio of 1.4 is an arbitrary cutoff, clasts below this ratio are sub-spherical, commonly difficult to measure, plot close to the origin on the hyperbolic net, and do not affect the determined opening angle of the hyperbola.

Traditionally the PHD method has been applied only to lineation-parallel planes with the assumption that deformation was monoclinic. We emphasize that choosing to analyze only the lineation-parallel plane does not make a deformation two-dimensional; much previous work has ignored the possible three-dimensionality of the strain history. More often than not deformations are three-dimensional. Previous kinematic vorticity studies investigating only lineation-parallel planes may have incorrectly assumed that the deformation in question could be treated as two-dimensional. To characterize three-dimensional deformations, ''two-dimensional'' analyses are commonly performed on multiple non-parallel sections to infer three-dimensional strain (Milton, 1980; Siddans, 1980; Owens, 1984; De Paor, 1990; Robin, 2002; Giorgis and Tikoff, 2004; Launeau and Robin, 2005).

4.2. Bootstrapping statistics

Bootstrapping is a statistical process that involves the creation of resampled ''bootstrap'' data sets that are treated as multiple data sets and meant to simulate the sampling of numerous samples when in actuality only one sample is available (Fig. 7; Diaconis and Efron, 1983; Mukul et al., 2004). Bootstrapping was introduced by Efron (1979) to evaluate distributions of data sets that were limited in size. Bootstrapping has recently been utilized by structural geologists to determine the error of the mean radial length of elliptical objects method for strain data (Mukul et al., 2004; Mulchrone et al., 2003).

For each sample, two data sets representing the lineation-normal and lineation-parallel planes were compiled from measurements of the three thin sections that defined each plane. Using the modified PHD method described earlier, only the ϕ angles of back-rotated grains were needed to define the kinematic vorticity number. The data sets were input into the computer program Statistica and a bootstrapping algorithm was applied. During each iteration of the bootstrapping process, a new data set with an equal number of entries to the initial data set was created by random sampling of the initial set (with replacement) (Fig. 7). During random sampling, any value can be sampled any number of times. Theoretically, reproducing the original data set is equally as likely as producing a data set composed entirely of a single value. For each plane, 200 bootstraps were done.

W_k-values for each iteration were dependant upon the maximum opening angle in the bootstrap data set. Because W_k-values are calculated using a cosine function, the scale is not linear. W_k-values can be converted to a linear scale by

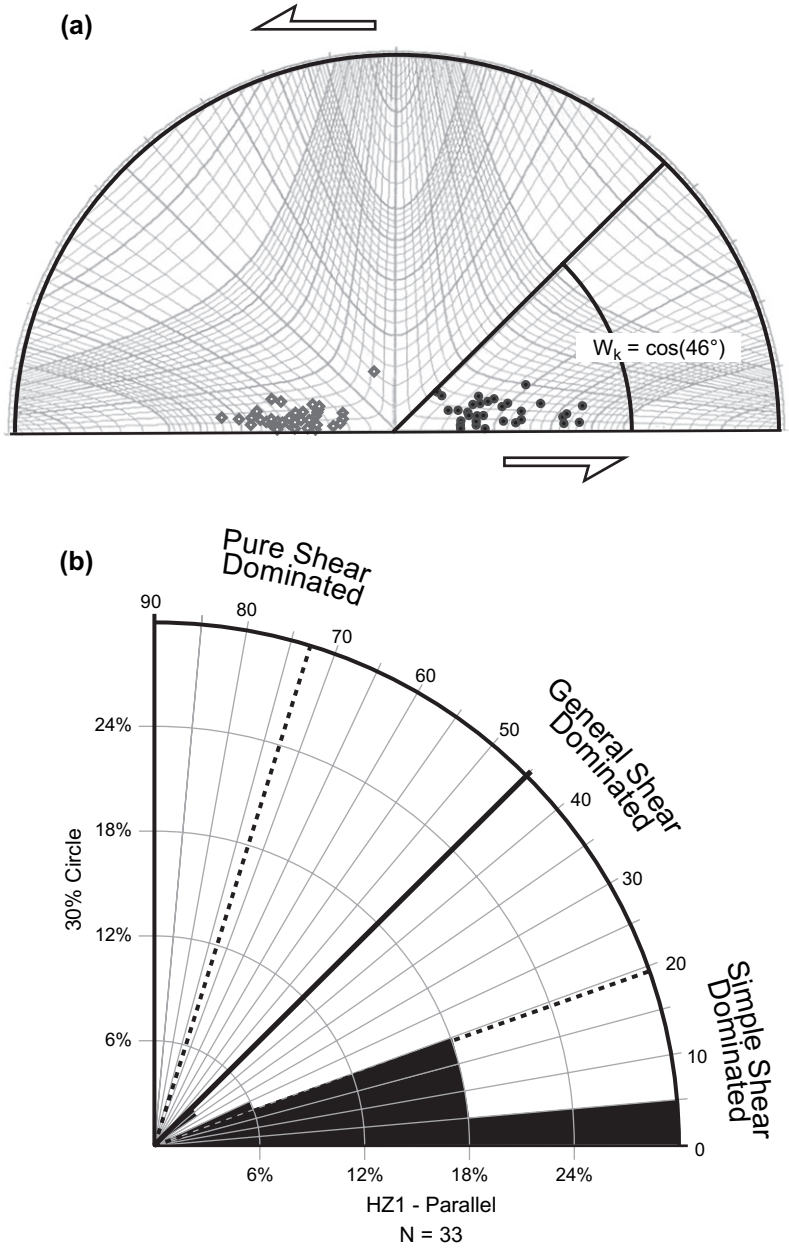

Fig. 6. Plot of data from sample HZ1 from the Hylas zone, Virginia. (a) Hyperbolic stereonet plot of axial ratios and long axis orientations of both forward and backward rotated porphyroclasts. Solid circles are backward rotated and hollow diamonds are forward rotated. (b) Radial distribution plot of backward rotated porphyroclasts with maximum opening angle defined by the solid black line.

considering the percent of a deformation resultant from simple shear (Fig. 1). In a single plane, a standard deviation was found for each of the 200 bootstrap-derived % simple shear values and then the average was calculated. The average values from each plane were used to calculate an average standard deviation for the PHD method.

4.3. ''Sieving'' the porphyroclasts

A form of computational ''sieving'' was applied to the data to test the significance of the axial ratio in determining the kinematic vorticity value. The use of the term sieving does not refer to any particular statistical method (at least that the authors are aware of), but rather was named as such because the procedure was reminiscent of the physical process of progressively sieving sediment samples. Sieving in this context simply refers to examining certain subsets of the data. Specifically, in the sieving process, back-rotated porphyroclasts are incrementally removed from consideration based on their axial ratio and then the orientations of the remaining grains were plotted on a radial distribution plot (Fig. 8). Rotation rate and sensitivity of porphyroclasts to changes in flow path is largely dependant upon the axial ratio of the porphyroclast (Passchier, 1987; Simpson and De Paor, 1993, 1997; Piazolo et al., 2002). Porphyroclasts with large axial ratios should be more sensitive to the flow path and orient sub-parallel to the stable positions. If

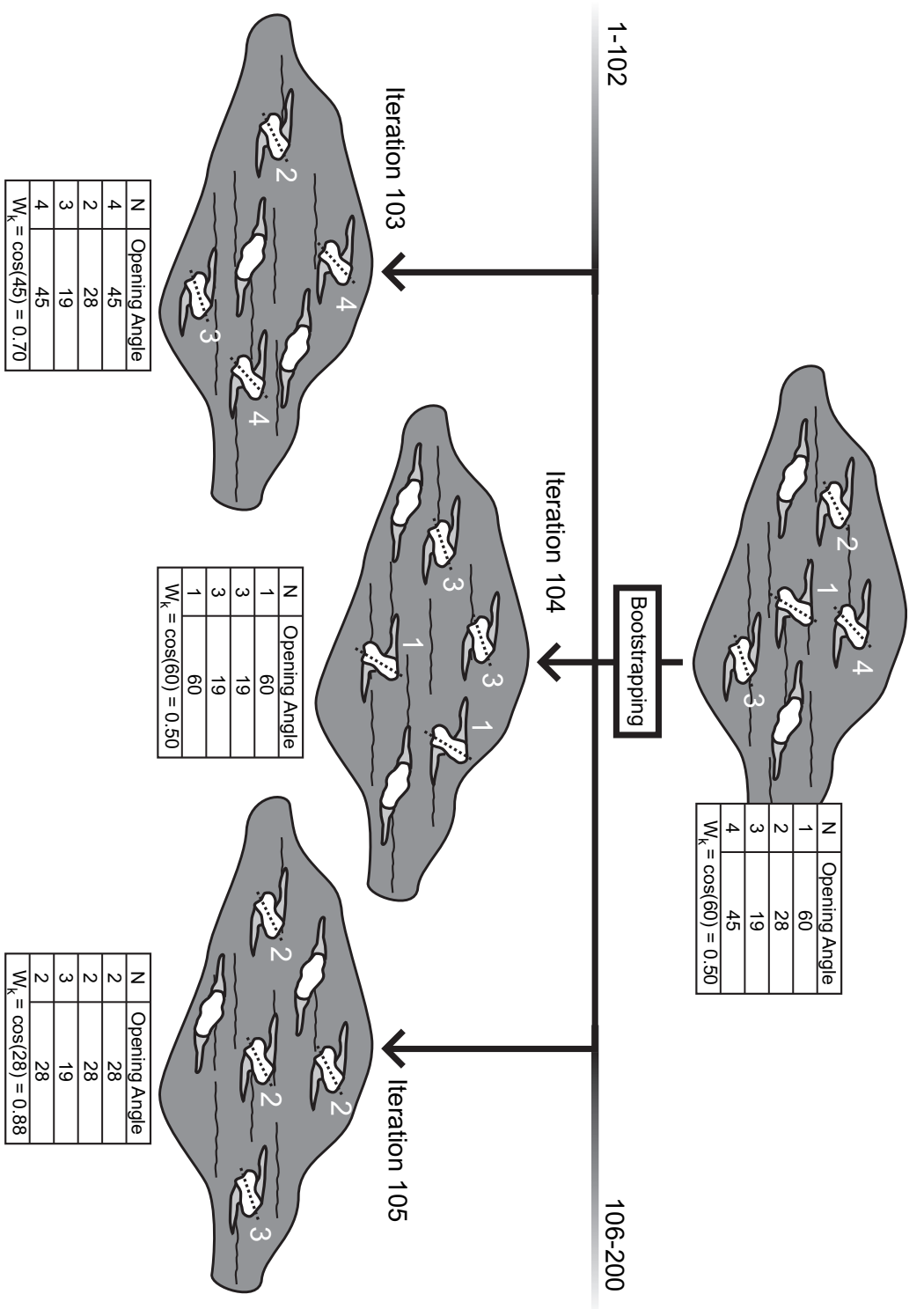

Fig. 7. The bootstrapping process begins with a single sample of orientations of backward rotated porphyroclasts. The bootstrapping algorithm generates multiple data sets produced by random sampling of the original data set. Bootstrapping simulates the collection of numerous new samples.

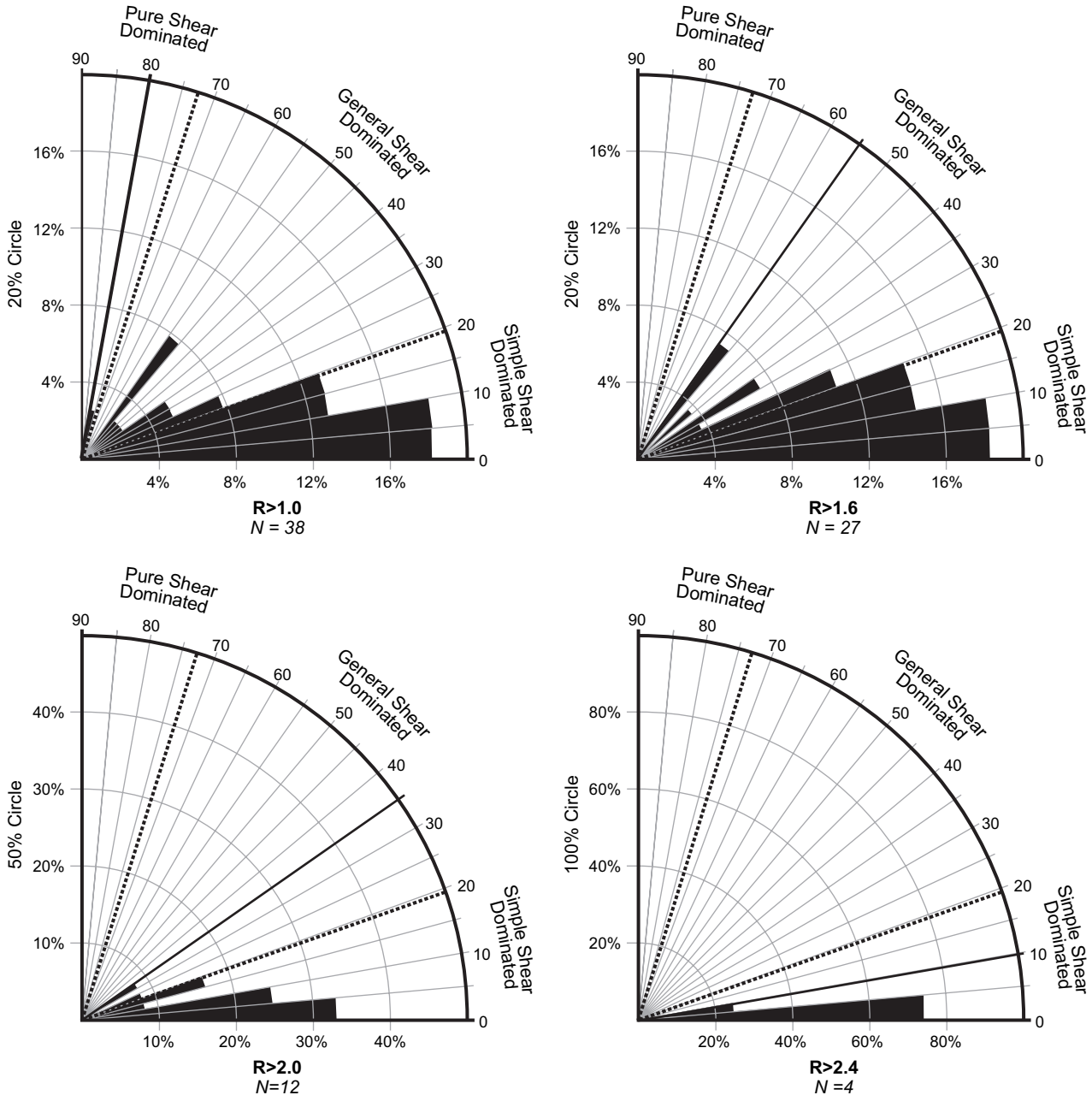

Fig. 8. Sieving plots of the lineation-parallel plane of sample AF01 from the Santa Catalina Mountains. Radial distribution plots were made incrementally removing axial ratios in 0.2 bins. Intermediates are not illustrated to show broad patterns, leaving plots of populations of grains with axial ratios greater than 1.0, 1.6, 2.0, and 2.4.

the extensional eigenvector is a stable position, as sieving continues, two populations should emerge within a group of porphyroclasts sub-parallel to foliation and an additional assemblage sub-parallel to the extensional eigenvector.

5. Results

5.1. Pusch Peak, Santa Catalina Metamorphic Core Complex, Arizona

Granitic rocks (Banks, 1980; Force, 1997) that comprise the Santa Catalina and Rincon Mountains in southern Arizona underwent significant ductile deformation during Tertiary crustal extension and metamorphic core complex formation (Davis, 1980; Rehrig and Reynolds, 1980). Pusch Peak, situated immediately north of Tucson, forms the westernmost exposure of the mylonitic rocks in the Santa Catalina Mountains. The protolith for these mylonitic rocks is a two-feldspar, garnet-bearing leucogranite and pegmatite that was intruded into older granites and metasedimentary rocks as a suite of sills (Force, 1997). Mylonitic rocks are characterized by a well-developed mineral elongation lineation that plunges 10–25° to the southwest. Strain is extremely localized, and a 1–3 m thick zone of ultramylonite crops out at the base of a pegmatite

sill along the southern flank of Pusch Peak. Naruk (1987) interpreted mylonitic deformation in the Santa Catalina forerange to be a product of simple shear, whereas Force (1997) later hypothesized that an early pure shear deformation was overprinted by later simple shearing.

Four samples of Pusch Peak ultramylonite were analyzed with the modified PHD method (Table 1). The ultramylonite matrix is very fine-grained quartz and muscovite with abundant feldspar porphyroclasts consistent with greenschist facies metamorphism (Fig. 9a, b). Feldspars underwent some crystal plastic deformation with many grains displaying undulose extinction and rare examples of deformation lamellae and subgrains but very minor recrystallization. Foliation is best developed in lineation-parallel planes and is not folded. In lineation-normal planes, the trace of foliation is still evident but poorly defined. At the slab and thin section scale, strong asymmetries are evident in both lineation-parallel and normal faces (Figs. 9a, b and 10).

Two samples, AF01 and AF02, yield W_k-values in the lineation-parallel section of 0.5–0.6, indicating general shear, and lineation-normal W_k-values of 0.3–0.4 (Table 1). The foliation is rarely folded and no relict fabrics are visible in thin section or hand sample, consistent with a single triclinic deformation rather than multiple monoclinic deformations that are overprinted to yield an apparent triclinic symmetry. A third sample from the Pusch Peak ultramylonites, SC5, yielded a lineation-parallel value of 0.03 and a normal value of 0.09, consistent with a pure shear dominated deformation (Table 1). Sample AF21 has a lineation-parallel W_k-value of 0.22 and a lineation-normal W_k-value of 0.09 indicating pure shear dominated deformation in both planes (Table 1).

5.2. Virgin Mountains

The Virgin Mountains are located in southeastern Nevada and northwestern Arizona in the Basin and Range province. Paleoproterozoic rocks (~1.7 Ga) that experienced regional deformation and metamorphism between 1650 and 1550 million years ago (Quigley et al., 2002) form the interior of the range and are overlain by a Paleozoic to Mesozoic cover sequence. The Virgin Mountains are part of the Mojave Precambrian complex, an upper-amphibolite to granulite facies metamorphic terrain (Quigley et al., 2002). Ductile strain in the Paleoproterozoic rocks in the Virgin Mountains has been interpreted to be the result of overall dextral strike-slip (transpressive), with significant strain partitioning into zones of pure shear dominated, simple shear dominated, and general shear dominated deformations (Quigley et al., 2002). Protoliths for the ultramylonites include a group of biotite-hornblende granodiorites, pelitic gneisses, and leucopegmatites (Quigley et al., 2002). Four samples were collected from the Cabin Canyon area of the Virgin Mountains where the mylonitic foliation is sub-vertical and the mineral elongation lineations plunge between 5 and 10°.

Samples AF08 and AF09 are petrographically identical and yield similar kinematic vorticity values (Table 1). The matrix is predominantly fine-grained recrystallized quartz with thin stringers of biotite and small amounts of well-aligned muscovite. Feldspar porphyroclasts are commonly elliptical with irregular grain boundaries and poorly defined tails of recrystallized quartz and feldspar (Fig. 9c, d). Feldspars commonly have undulose extinction, rare deformation lamellae, and are mantled by neoblasts, consistent with lower amphibolite facies conditions (Fig. 9c, d). Average W_k-values for both the lineation-parallel and lineation-normal sections are 0.10, consistent with a pure shear dominated deformation (Table 1). Both samples AF08 and AF09 were large enough to be sectioned along planes at 30° and 60° from the lineation-parallel plane. The W_k-values from these sections are also consistent with a pure shear dominated deformation (Table 1). Samples AF06 and AF07 are petrographically distinct, with respect to samples AF08 and AF09, and composed of approximately equal amounts fine-grained quartz, biotite and muscovite that define a strong foliation. Feldspar porphyroclasts, are elliptical with well-defined grain boundaries, and rarely display undulose extinction (Fig. 9e, f). Both AF06 and AF07 yield W_k-values of 0.1–0.2 for the lineation-parallel plane and values of 0.4 for the lineation-normal plane (Table 1).

The Cabin Canyon segment of the Virgin Mountains was interpreted to be a zone of Paleoproterozoic transpressional dextral strike-slip deformation (Quigley et al., 2002). The kinematic vorticity values in samples AF06 and AF07 are much higher in the lineation-normal plane, consistent with a "rolling lineation" parallel to the vorticity vector (Sanderson and Marchini, 1984; Passchier, 1998; Tikoff and Greene, 1997). However, given the sectional uncertainty, this could be described as a triclinic fabric. Lineations in Virgin Mountain ultramylonites plunge shallowly and Quigley et al. (2002) used the lineation orientation as an indicator of strike-slip tectonics. However, if the lineation is a rolling lineation, then the transport direction is orthogonal to the lineation, implying that these zones are not strike-slip, but rather experienced high-angle dip-slip general shear deformation (Fig. 11). Quigley et al. (2002) discussed the presence of sense of shear indicators on the lineation-normal faces of ultramylonites, but interpreted these indicators to be the result of an earlier thrusting episode. Our vorticity data are inconsistent with significant strike-slip movement in these ultramylonites. The relatively low W_k-values for the lineation-parallel planes indicate that the deformation was nearly monoclinic with a transpressive geometry (Fig. 5). The other two Virgin Mountain samples, AF08 and AF09, are likely from a zone of pure shear dominated strain. This observation is supported by pure shear dominated W_k-values for both the lineation-normal, lineation-parallel, and intermediate planes of the samples.

5.3. Hylas zone

The Hylas zone is a regional-scale, northeast–southwest striking zone of mylonitic rocks in the Virginia Piedmont (Bobyarchick and Glover, 1979). Mesoproterozoic to Paleozoic gneisses, amphibolites, and granites form the protoliths for Hylas zone tectonites (Bobyarchick and Glover, 1979; Gates and Glover, 1989). Gates and Glover (1989) provide thermochronologic evidence for a progressive lower amphibolite to greenschist facies deformation event that began at ~330 Ma and was followed by steady cooling into the Mesozoic. Hylas

Table 1
Kinematic vorticity values broken down by thin section, with values presented as W_k-values and percent simple shear

	Section	W_k	± Error	% Simple	SD	N
Santa Catalina						
AF01	PA	0.72	0.10	52		7
	PB	0.57	0.12	39		19
	PC	0.64	0.11	44		7
	Parallel	0.57	0.12	39	3	33
	NA	0.37	0.13	24		10
	NB	0.82	0.08	61		10
	NC	0.90	0.06	71		12
	Normal	0.37	0.13	24	18	32
AF02	PA	0.56	0.12	38		18
	PB	0.66	0.11	46		12
	PC	0.77	0.09	56		13
	Parallel	0.56	0.12	38	5	43
	NA	0.59	0.11	40		25
	NB	0.28	0.14	18		17
	NC	0.63	0.11	43		15
	Normal	0.28	0.14	18	9	57
SC5	PA	0.37	0.13	24		24
	PB	0.48	0.13	32		10
	PC	0.03	0.14	2		24
	Parallel	0.03	0.14	2	13	58
	NA	0.69	0.11	49		19
	NB	0.09	0.14	6		25
	NC	0.48	0.13	32		25
	Normal	0.09	0.14	6	14	69
AF21	PA	0.92	0.06	74		14
	PB	0.22	0.14	14		9
	PC	0.95	0.04	80		10
	Parallel	0.22	0.14	14	18	33
	NA	0.7	0.10	49		15
	NB	0.66	0.11	46		17
	NC	0.09	0.14	6		17
	Normal	0.09	0.14	6	15	49
Virgin Mountain						
AF06	PA	0.74	0.10	53		5
	PB	0.10	0.14	6		19
	PC	0.47	0.13	31		16
	Parallel	0.10	0.14	6	7	40
	NA	0.85	0.08	65		12
	NB	0.67	0.11	47		15
	NC	0.39	0.13	26		18
	Normal	0.39	0.13	26	9	45
AF07	PA	0.19	0.14	12		17
	PB	0.54	0.12	36		8
	PC	0.54	0.12	36		11
	Parallel	0.19	0.14	12	10	36
	NA	0.82	0.08	62		11
	NB	0.44	0.13	29		24
	NC	0.41	0.13	27		16
	Normal	0.41	0.13	27	5	51
AF08	PA	0.33	0.14	21		14
	PB	0.71	0.10	50		13
	PC	0.14	0.14	9		16
	Parallel	0.14	0.14	9	9	43
	30-A	0.09	0.14	6		23
	30-B	0.59	0.12	40		22
	30-C	0.12	0.14	8		34
	30-Int	0.09	0.14	6	9	79
	60-A	0.14	0.14	9		30
	60-B	0.48	0.13	32		34
	60-C	0.03	0.14	2		19
	60-Int	0.03	0.14	2	10	83
	NA	0.68	0.11	48		9
	NB	0.02	0.14	1		18
	NC	0.03	0.14	2		25
	Normal	0.02	0.14	1	3	52
AF09	PA	0.17	0.14	11		24
	PB	0.09	0.14	6		26
	PC	0.05	0.14	3		43
	Parallel	0.05	0.14	3	2	93
	30-A	0.67	0.11	47		21
	30-B	0.48	0.13	32		25
	30-C	0.29	0.14	19		14
	30-Int	0.29	0.14	19	6	60
	60-A	0.09	0.14	6		12
	60-B	0.54	0.12	36		10
	60-C	0.47	0.13	31		11
	60-Int	0.09	0.14	6	14	33
	NA	0.29	0.14	19		24
	NB	0.17	0.14	11		24
	NC	0.79	0.09	58		19
	Normal	0.17	0.14	11	3	67
Hylas zone						
HZ1	PA	0.72	0.10	51		16
	PB	0.95	0.04	80		9
	PC	0.93	0.05	76		8
	Parallel	0.72	0.10	51	8	33
	NA	0.75	0.10	54		4
	NB	0.93	0.05	76		8
	NC	0.72	0.10	51		8
	Normal	0.72	0.10	51	3	20

Values are only considering grains with axial ratios greater than 1.4 but have not been sieved. Error values (±Error) for each plane are given for the W_k-values based on the bootstraps. Also included are the standard deviations in percent simple shear (SD) for planes based on the bootstraps. *N* is the number of back-rotated porphyroclasts (with axial ratios greater than 1.4) analyzed in each plane.

mylonites and ultramylonites are interpreted to be the product of dextral strike-slip movement (Bobyarchick and Glover, 1979; Gates and Glover, 1989). We analyzed one sample from the Royal Stone quarry in Rockville, Virginia. The matrix is predominantly fine-grained quartz and white mica with abundant epidote-rich zones consistent with greenschist facies metamorphism (Fig. 9g, h). Porphyroclasts are rare and commonly composed of microcline with poorly defined tails of recrystallized quartz (Fig. 9g, h). Kinematic vorticity values

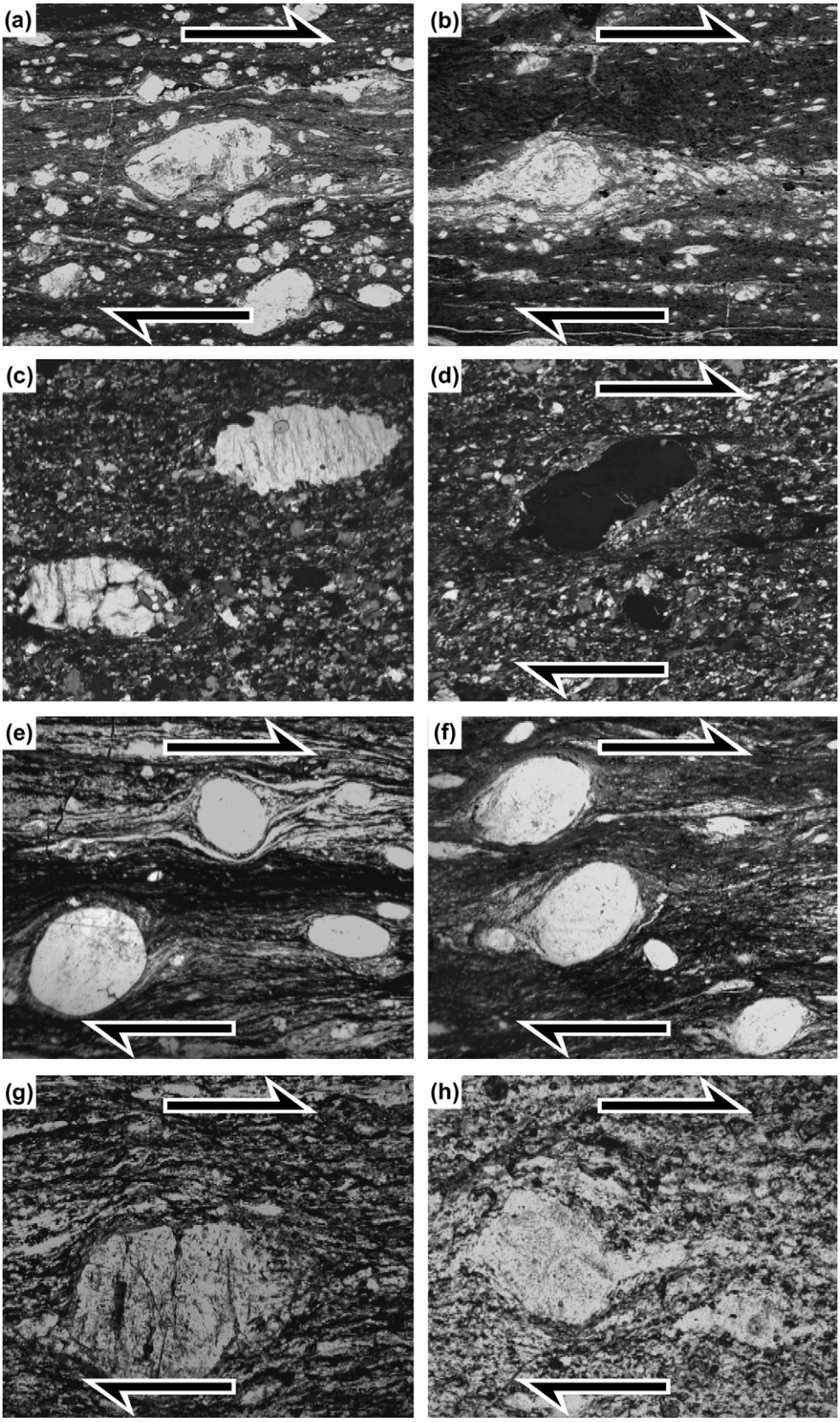

Fig. 9. Photomicrographs of ultramylonites with sense of shear (when it was determinable) illustrated with white arrows, base of images are 3.4 mm wide. (a) PPL image of lineation-parallel plane of sample SC5 from the Santa Catalina Mountains. (b) PPL image of lineation-normal plane of sample AF01 from the Santa Catalina Mountains. (c) XPL image of lineation-parallel plane of sample AF09 from the Virgin Mountains. (d) XPL image of lineation-normal plane of sample AF08 from the Virgin Mountains. (e) PPL image of lineation-parallel plane of sample AF06 from the Virgin Mountains. (f) PPL image of lineation-normal plane from sample AF06 of the Virgin Mountains. (g) PPL image of lineation-parallel plane of sample HZ1 from the Hylas zone. (h) PPL image of lineation-normal plane of sample HZ1 from the Hylas zone.

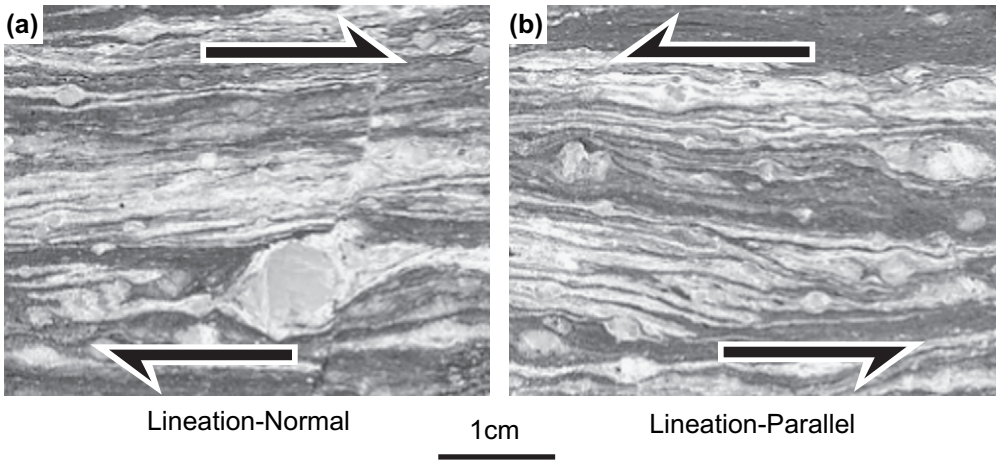

Fig. 10. Ultramylonite slab from the Santa Catalina Mountains. Sense of shear markers in both lineation-normal and parallel planes are very well defined. (a) Lineation-normal plane exhibiting clear top to the right sense of shear. (b) Lineation-parallel plane with top to the left sense of shear. Strong sense of shears in both planes could indicate a triclinic deformation.

for the Hylas zone sample indicate general shear in both the lineation-normal and lineation-parallel planes with both planes yielding a W_k-value of 0.72 (Table 1). Vorticity data are consistent with general shear deformation with a triclinic symmetry. Furthermore, foliation-parallel quartz ribbons exhibit strong grain-shape asymmetries and oblique fabrics in both lineation-parallel and lineation-normal sections (Fig. 12). The thermochronologic evidence of Gates and Glover (1989) as well as the lack of microstructural evidence for multiple deformation events implies a single general shear deformation that may be triclinic.

5.4. Error estimation from bootstraps

Bootstrapping data is best visualized as a radial distribution of the maximum opening angles reported from each iteration of the bootstrap (Fig. 13). On average, the lowest W_k-value from a plane was reported 70% of the time, so the largest petal on the radial distribution plot was always the outlying petal. The lowest value is considered the accepted value because the most extreme outlier typically defines the measurement yielded from the PHD method. The other 30% of measurements give a lower opening angle and so correspondingly a higher, more simple shear dominated, W_k-value. Usually, the distributions of opening angles are within 15°, but some analyses produced wider distributions with opening angle disparities of between 20 and 50°.

The average of the standard deviations from all of the bootstraps gives a 1σ standard error of $\pm 9\%$ for a W_k-value measured on a percent simple shear scale. Error bars from the percent simple shear scale convert to error bars for specific W_k-values and range from ± 0.14 for end member pure shear to ± 0.01 for end member simple shear (Fig. 14). The percent simple shear error value is based on the average values of bootstraps done on lineation-parallel planes, lineation-normal planes, and the intermediate planes analyzed. The error value is $\pm 8\%$ simple shear if only considering bootstraps of lineation-parallel planes. The error values for lineation-normal planes and intermediate planes are higher, at $\pm 9\%$ and $\pm 10\%$, respectively.

Simpson and De Paor (1997) suggest that the accuracy of the PHD increases with the number of back-rotated porphyroclasts measured. To test this idea, correlation between error and number of back-rotated porphyroclasts was calculated with a Pearson correlation function. The data set consisted of 22 pairs (one for each plane composed of three thin sections) of the number of back-rotated porphyroclasts identified in the plane and the standard error found for that plane with the bootstrapping statistics. A slight negative correlation exists, meaning that as the number of grains went up the error went down, as expected, but this correlation was not statistically significant with a p-value of 0.385. This suggests that the number of grains analyzed does not appreciably improve the accuracy of the analyses. Analyzing as many grains as possible is still recommended because this should increase the likelihood of finding outlying grains that define the analysis.

5.5. Axial ratio sieving

Porphyroclasts with axial ratios less than 2.0 typically define a nearly random assortment of long axis orientations (Fig. 8). Most grains and the variability in long axis orientations is removed from the data set when only considering porphyroclasts with axial ratios greater than 2.0. Typically, porphyroclasts with axial ratios between 2.0 and 3.0 define several sets of orientations of long axes, but these populations are not oriented at the corresponding opening angle that defines the kinematic vorticity number that is determined by the PHD method for the plane in question. Above 3.0, porphyroclasts are approximately parallel to the foliation plane, with an opening angle at maximum 20°, indicating a minimum kinematic vorticity number of 0.93 (75% simple shear).

6. Discussion

The PHD results are inconsistent at both the shear zone and hand sample scale. Kinematic vorticity values from samples within the same shear zone indicate different styles of shear

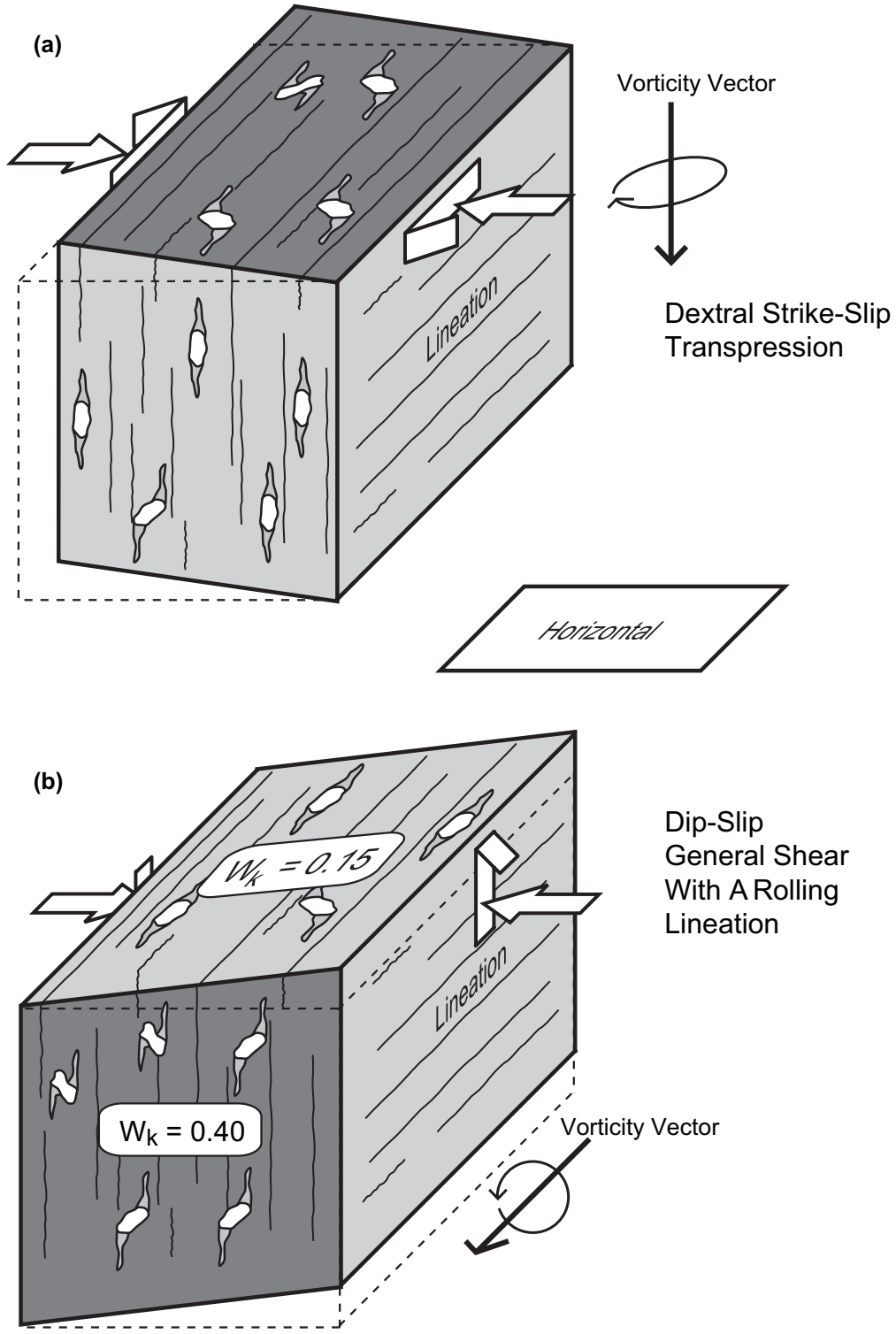

Fig. 11. (a) Hypothetical strain geometry in the Virgin Mountain ultramylonites as interpreted by Quigley et al. (2002). The ultramylonites were theorized to be the product of dextral strike-slip transpression with the slip direction being parallel to the nearly horizontal lineation. (b) Based on kinematic vorticity analysis, the lineation may be a rolling lineation defining the ultramylonites as a product of dip-slip general shear. Note: that for both figures the dotted lines do not represent initial shapes, but rather provide reference for visualizing the three-dimensional object shapes.

(Table 1). Piazolo et al. (2002) suggested that kinematic vorticity may be very locally dependent and that the kinematic vorticity number for any sample may be significantly different from the kinematic vorticity number of the bulk flow. Variability in results between values from different locations in the respective shear zones may be a function of this local unevenness of vorticity (strain partitioning), rather than a problem with the PHD method. W_k-values from a single hand sample should not be

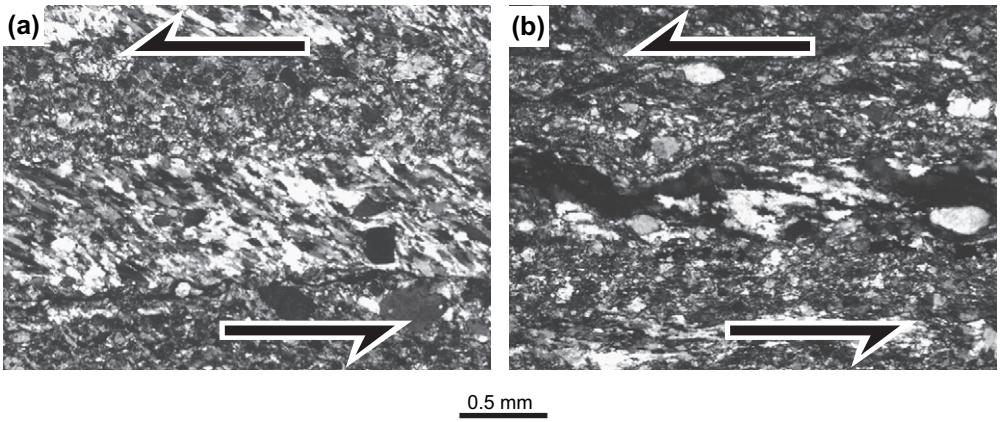

Fig. 12. Foliation-parallel quartz vein in sample HZ1 from the Hylas zone, Virginia. (a) XPL photomicrograph of lineation-normal plane. The quartz vein has a very strong preferred orientation of the long axes of recrystallized grains. The long axes are inclined with the sense of shear, the high angle between the quartz long axes and the foliation plane is consistent with a widening shear zone during the last increments of deformation. (b) XPL photomicrograph of lineation-parallel plane. Long axes or recrystallized quarts is also inclined with sense of shear, but not as strongly as in the lineation-normal plane.

considered indicative of the W_k of the entire zone and instead samples should be analyzed from several spaced locations in the shear zone.

Kinematic vorticity numbers of thin sections from the same plane of a hand sample also vary significantly. For example, three W_k-values from three thin sections defining the lineation-parallel plane of AF06 were 0.74, 0.47, and 0.10. The first and second values both indicate general shear, but with significant differences in shortening normal to the foliation. The final value indicates a pure shear dominated deformation. The variability in flow responsible for preserving W_k-values of 0.74 (53% simple shear) and 0.10 (6% simple shear) a few centimeters apart in a deforming ultramylonite would render meaningful W_k analysis nearly impossible. Uncertainties in the PHD method more easily explain the unpredictability of W_k-values within a single plane. Error ranges derived from the bootstrapping statistics indicate a certain amount of inherent error in the PHD method, but not enough to explain the variability seen in the analyses. Reliance on the outlying back-rotated porphyroclast that defines the kinematic vorticity number may contribute to the imprecision found in the PHD method.

When reporting the kinematic vorticity value for any planes, because of the nature of the PHD, the lowest value (and correspondingly the highest opening angle) is reported. Kinematic vorticity values as determined by the PHD are dependent upon the most extreme outlier within the data set. In cases such as sample AF21 from the Santa Catalinas, the outlier dramatically changes the W_k-values. The reported value from the lineation-parallel plane is 0.22, but all of the back-rotated porphyroclasts, with the exception of four of the 40 grains would yield a W_k-value of greater than 0.90. The W_k-value from the normal plane of AF21 (0.09) is based solely on one outlying grain, the next most outlying porphyroclast yielding a W_k-value of 0.45. Simpson and De Paor (1997) advised that if the outlying grain plotted at an orientation on the hyperbolic net significantly different from the rest of the population, it should be considered suspect. The bootstraps contained all grains to test the significance of the outlying grain and as reported earlier, the bootstraps returned this outlier (or a porphyroclast with a ϕ angle within 5° of the outlier), on average, 70% of the time. This would indicate that the outlying grain is significant, but does not preclude the idea that the outlier may not accurately represent the kinematic vorticity value and instead may be a product of cut effects, the initial orientation and shape of the porphyroclast or an indicator of the three-dimensional nature of the flow.

Bootstraps indicate that outlying grains are significant, but do outliers define the extensional eigenvector? Sieving results indicate that large axial ratio back-rotated sigma porphyroclasts, the grains expected to be above the critical axial ratio, do not track the extensional eigenvector and instead are oriented sub-parallel to the foliation plane (Fig. 8). We interpret the sieves as evidence that the extensional eigenvector does not act as a strong fabric attractor. The uncertainty inherent in the method as identified by the bootstraps prevents the PHD from being useful in providing specific kinematic vorticity numbers. Error bars as large as ± 0.14 are quite significant when the effective scale of W_k-values are 0 to 1 and a small change in kinematic vorticity can yield a large change of foliation-normal thinning estimates. In spite of these uncertainties, the PHD method can discriminate between pure shear dominated, general shear, and simple shear dominated deformations. Ability to distinguish between types of shear is useful as a method for characterizing strain symmetry. Many of the samples analyzed in this study preserve fabrics that are best explained by a triclinic deformation symmetry. If it is clear that general or simple shear conditions existed in both the lineation-parallel and normal planes then the deformation is triclinic. Analysis of several key planes at different orientations with the PHD method is a viable method for strain symmetry analysis.

7. Conclusions

The porphyroclast hyperbolic distribution method of vorticity analysis has significant limitations and is not a reliable method for determining W_k-values with high precision. However, the

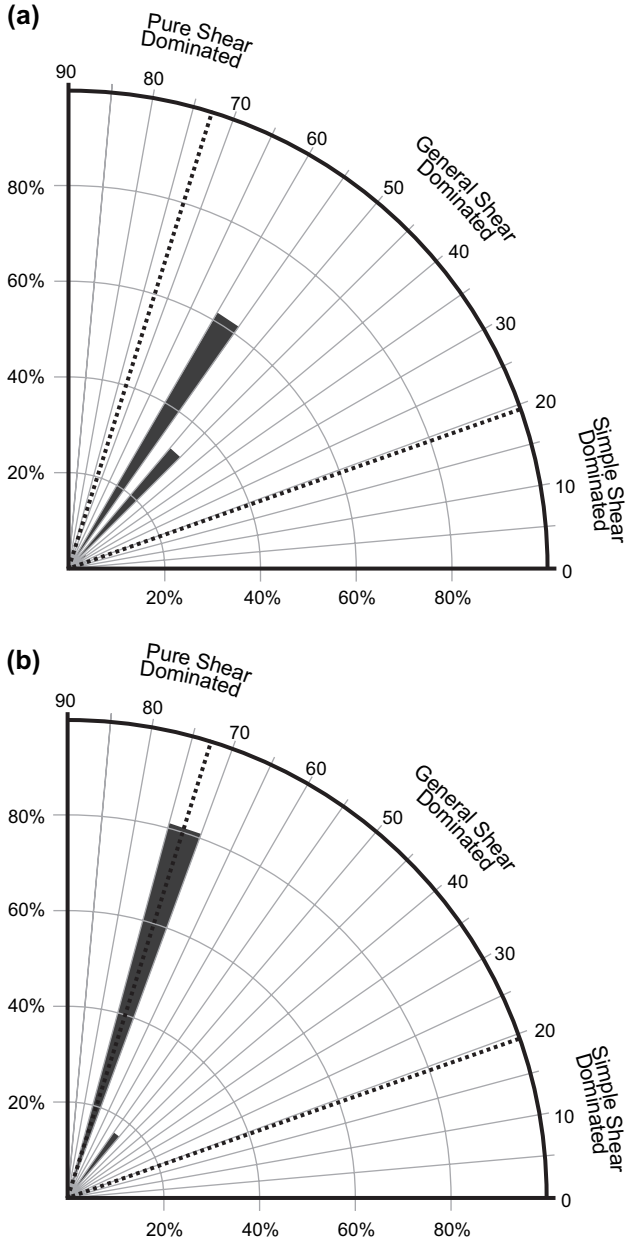

Fig. 13. Radial distribution of the bootstrap results for sample AF02 from the Santa Catalina Mountains. Petals represent the opening angle indicated by the most extreme outlier returned by iterations of the bootstrap. (a) Plot for the bootstraps of the lineation-parallel section of AF02. As indicated by the radius of the petal, 60% of the bootstraps included this outlying grain, while the other 40% did not include this grain and the PHD analysis of these data sets yielded a higher kinematic vorticity number. (b) Plot of the bootstraps for the normal section of AF02. Eighty percent of the bootstraps included an outlying grain with a long axis orientation of between 70 and 75° (as measured from the foliation plane).

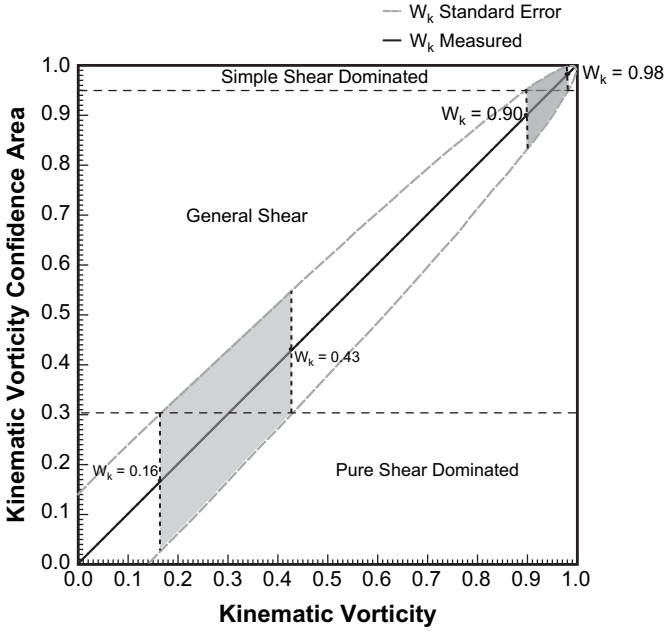

Fig. 14. Graph of the error fluctuation in W_k space. Because the error is calculated on a linear scale and then converted to a non-linear scale, the error value varies with a max at a W_k-value of 0 and its minimum near a W_k-value of 1.0. Shaded areas are W_k-values whose error bars extend into two zones of shear types.

PHD method is useful for discriminating between simple shear dominated, pure shear dominated, and general shear deformations. Furthermore, the modified PHD method, as described in this paper, is useful for discerning triclinic shear from monoclinic shear. Although past PHD studies have essentially assumed monoclinic flow, PHD analysis of multiple planes provides aviable test of the two-dimensionality of the strain symmetry. The PHD method identified ultramylonites from the Pusch Peak region in the Santa Catalina metamorphic core complex as the product of triclinic general shear. Additionally, ultramylonites from the Cabin Canyon region in the Virgin Mountains may have experienced dip-slip general shear to pure shear dominated deformation, not dextral strike-slip deformation as previously reported. An ultramylonite from the Hylas zone is the product of triclinic general shear.

To better understand the ability of the PHD method to identify triclinic shear, several tasks should be completed. The PHD method should be used to analyze lineation-normal and lineation-parallel planes from shear zones that have been independently determined to have a monoclinic or triclinic symmetry. Further study of kinematic vorticity in triclinically deformed rocks will require a more three-dimensional approach. Analyzing a lineation-parallel plane alone is incomplete and even with the addition of a lineation-normal plane the analysis is still limited. The examination of the intermediate planes is still a viable idea, and should be expanded to analyze as many planes as physically possible between the lineation-normal and lineation-parallel planes. When the technology becomes more feasible and readily available, the analysis of populations of porphyroclasts should be done with tomography to produce a true three-dimensional representation of the fabric (Carlson et al., 1998; Carlson et al., 2003; Ketcham, 2005).

Acknowledgements

This work was supported by the Roy R. Charles center and a Faculty Research leave granted to C.M. Bailey by the

College of William & Mary. J. Spencer is thanked for introducing the authors to the ultramylonites in the Santa Catalinas and T. Brazell is thanked for granting access to the Royal Stone Quarry in Rockville, VA. R. Lockwood is thanked for helpful discussions regarding the bootstrapping statistics and S. Giorgis is thanked for beneficial conversations regarding the use of the PHD method. Finally, S. Wallis, S. Coelho, P. Xypolias, and K. Mulchrone are thanked for their reviews of previous versions of this manuscript.

References

Bailey, C.M., Bobyarchick, A., Jiang, D., 2002. Kinematics and vorticity of high-strain zones, Virginia Blue Ridge and Piedmont. Geological Society of America Field Forum, 26 (April 26–21st 2002).

Bailey, C.M., Eyster, E.L., 2003. General shear deformation in the Pinaleno Mountains metamorphic core complex, Arizona. Journal of Structural Geology 25, 1883–1892.

Bailey, C.M., Francis, B.E., Fahrney, E.E., 2004. Strain and vorticity analysis of transpressional high-strain zones from the Virginia Piedmont, USA. In: Aslop, G.I., Holdsworth, R.E., McCaffrey, K.J.H., Hand, M. (Eds.), Flow Processes in Faults and Shear Zones. Geological Society, Special Publications, vol. 224, pp. 249–264.

Bailey, C.M., Polvi, L.E., Forte, A.M., 2007. Pure shear dominated high-strain zones in basement terranes. In: 4-D Framework of Continental Crust. Geological Society of America Memoir.

Banks, N.G., 1980. Geology of a zone of metamorphic core complexes in southeastern Arizona. In: Crittenden, M.D., Coney, P.J., Davis, G.H. (Eds.), Cordilleran Metamorphic Core Complexes. Geological Society of America Memoir, vol. 153, pp. 177–215.

Bobyarchick, A., 1986. The eigenvalues of steady state flow in Mohr space. Tectonophysics 122, 35–51.

Bobyarchick, A.R., Glover III, L., 1979. Deformation and metamorphism in the Hylas zone and adjacent parts of the eastern Piedmont in Virginia. Geological Society of America Bulletin 90, 739–752.

Carlson, W.D., Denison, C., Ketcham, R.A., 1998. Visualization, interpretation, and quantitative analysis of rock textures in three dimensions using high resolution X-ray computed tomography. EOS, Transactions, American Geophysical Union 17, 355.

Carlson, W.D., Rowe, T., Ketcham, R.A., Colbert, M.W., 2003. Applications of high-resolution X-ray computed tomography in petrology, meteorics and paleontology. In: Geological Society, Special Publications, vol. 215, pp. 7–22.

Davis, G.H., 1980. Structural characteristics of metamorphic core complexes, southern Arizona. In: Crittenden, M.D., Coney, P.J., Davis, G.H. (Eds.), Cordilleran Metamorphic Core Complexes. Geological Society of America Memoir, vol. 153, pp. 35–77.

De Paor, D.G., 1988. R_f/Phi_f strain analysis using an orientation unit. Journal of Structural Geology 10, 323–333.

De Paor, D.G., 1990. Determination of the strain ellipsoid from sectional data. Journal of Structural Geology 12, 131–137.

Diaconis, P., Efron, B., 1983. Computer-intensive methods in statistics. Scientific American 248, 116–130.

Efron, B., 1979. Bootstrap methods: another look at the jackknife. The Annals of Statistics 7, 1–26.

Force, E.R., 1997. Geology and Mineral Resources of the Santa Catalina Mountains, Southeastern Arizona. Center for Mineral Resources, the University of Arizona, The U.S. Geological Survey, Tucson.

Fossen, H., Tikoff, B., 1993. The deformation matrix for simultaneous simple shearing, pure shearing and volume change, and its application to transpression–transtension tectonics. Journal of Structural Geology 15, 413–422.

Gates, A.E., Glover III, L., 1989. Alleghanian tectono-thermal evolution of the dextral transcurrent Hylas Zone, Virginia Piedmont, USA. Journal of Structural Geology 11, 407–419.

Ghosh, S.K., 1987. Measure of non-coaxiality. Journal of Structural Geology 9, 111–113.

Ghosh, S.K., Ramberg, H., 1976. Reorientation of inclusions by combination of pure and simple shear. Tectonophysics 34, 1–70.

Giorgis, S., Tikoff, B., 2004. Constraints on kinematics and strain from feldspar porphyroclast populations. In: Aslop, G.I., Holdsworth, R.E., McCaffrey, K.J.H., Hand, M. (Eds.), Flow Processes in Faults and Shear Zones. Geological Society, Special Publications, vol. 224, pp. 83–99.

Jezek, J., Schulman, K., Segeth, K., 1996. Fabric evolution of rigid inclusions during mixed coaxial and simple shear flows. Tectonophysics 257, 203–221.

Jiang, D., Williams, P.F., 1998. High strain zones: a unified model. Journal of Structural Geology 20, 1105–1120.

Ketcham, R.A., 2005. Computational methods for quantitative analysis of three-dimensional features in geological specimens. Geosphere 1, 32–41.

Law, R.D., Searle, M.P., Simpson, R.L., 2004. Strain, deformation temperatures and vorticity of flow at the top of the Greater Himalayan Slab, Everest Massif, Tibet. Journal of the Geological Society of London 161, 305–320.

Launeau, P., Robin, P.F., 2005. Determination of fabric and strain ellipsoids from measured sectional ellipses – implementation and applications. Journal of Structural Geology 27, 2223–2233.

Lin, S., Jiang, D., 2001. Using along-strike variation in strain and kinematics to define the movement direction of curved transpressional shear zones: an example from northwestern Superior Province, Manitoba. Geology 29, 767–770.

Lin, S., Jiang, D., Williams, P.F., 1998. Transpression (or transtension) zones of triclinic symmetry: natural example and theoretical modeling. In: Holdsworth, R.E., Strachan, R.A., Dewey, J.F. (Eds.), Continental transpressional and transtensional tectonics. Geological Society, Special Publications, vol. 135, pp. 41–57.

Means, W.D., Hobbs, B.E., Lister, G.S., Williams, P.F., 1980. Vorticity and non-coaxiality in progressive deformations. Journal of Structural Geology 2, 371–378.

Milton, N.J., 1980. Determination of the strain ellipsoid from measurements on any three sections. Tectonophysics 64, T19–T27.

Mukul, M., Roy, D., Satpathy, S., Kumar, V.A., 2004. Bootstrapped spatial statistics: a more robust approach to the analysis of finite strain data. Journal of Structural Geology 26, 595–600.

Mulchrone, K.F., Grogan, S., Prithwijit, D., 2005. The relationship between magmatic tiling, fluid flow and crystal fraction. Journal of Structural Geology 27, 179–197.

Mulchrone, K.F., O'Sullivan, F., Meere, P.A., 2003. Finite strain estimation using the mean radial length of elliptical objects with bootstrap confidence intervals. Journal of Structural Geology 25, 529–539.

Naruk, S.J., 1987. Kinematic significance of mylonitic foliation. Ph.D thesis, University of Arizona.

Owens, W.H., 1984. The calculation of a best-fit ellipsoid from elliptical sections on arbitrarily oriented planes. Journal of Structural Geology 6, 571–578.

Passchier, C.W., 1987. Stable positions of rigid objects in non-coaxial flow – a study in vorticity analysis. Journal of Structural Geology 9, 679–690.

Passchier, C.W., 1988. Analysis of deformation paths in shear zones. Geologische Rundschau 77, 309–318.

Passchier, C.W., 1997. The fabric attractor. Journal of Structural Geology 19, 113–127.

Passchier, C.W., 1998. Monoclinic model shear zones. Journal of Structural Geology 20, 1121–1137.

Piazolo, S., Bons, P.D., Passchier, C.W., 2002. Influence of matrix rheology and vorticity on fabric development of populations of rigid objects during plane strain deformation. Tectonophysics 351, 315–329.

Quigley, M.C., Karlstrom, K.E., Beard, S., Bohannon, B., 2002. Influence of proterozoic and laramide structures on the Miocene extensional strain filed, North Virgin Mountains, Nevada/Arizona. In: Geological Society of America Rocky Mountain Section Annual Meeting, Cedar City, Utah.

Rehrig, W.A., Reynolds, S.J., 1980. Geologic and geochronologic reconnaissance of a northwest-trending zone of metamorphic core complexes in southern and western Arizona. In: Crittenden, M.D., Coney, P.J., Davis, G.H. (Eds.), Cordilleran Metamorphic Core Complexes. Geological Society of America Memoir, 153, pp. 131–175.

Robin, P.F., 2002. Determination of fabric and strain ellipsoids from measured sectional ellipses – theory. Journal of Structural Geology 24, 531–544.

Robin, P.F., Cruden, A.R., 1994. Strain and vorticity patterns in ideally ductile transpression zones. Journal of Structural Geology 16, 447–466.

Sanderson, D.J., Marchini, W.R.D., 1984. Transpression. Journal of Structural Geology 6, 449–458.

Siddans, A.W.B., 1980. Analysis of three-dimensional, homogenous, finite strain using ellipsoidal objects. Tectonophysics 64, 1–16.

Simpson, C., De Paor, D.G., 1993. Strain and kinematic analysis in general shear zones. Journal of Structural Geology 15, 1–20.

Simpson, C., De Paor, D.G., 1997. Practical analysis of general shear zones using the porphyroclast hyperbolic distribution method: an example from the Scandinavian Caledonides. In: Sengputta, S. (Ed.), Evolution of Geological Structures in Micro- to Macro-Scales, pp. 169–184.

Tikoff, B., Fossen, H., 1995. The limitations of three dimensional kinematic vorticity analysis. Journal of Structural Geology 17, 1771–1784.

Tikoff, B., Greene, D., 1997. Stretching lineations in transpressional shear zones; an example from the Sierra Nevada Batholith, California. Journal of Structural Geology 19, 29–39.

Truesdell, C., 1953. Two measures of vorticity. Journal of Rational Mechanics and Analysis 2, 173–217.

Vissers, R.L.M., 1987. The effect of foliation orientation on the inferred rotation axes and rotation angles of rotated porphyroclasts. Tectonophysics 139, 275–283.

Wallis, S.R., 1992. Vorticity analysis in a metachert from the Sanbagawa belt, SW Japan. Journal of Structural Geology 14, 271–280.

Wallis, S.R., 1995. Vorticity analysis and recognition of ductile extension in the Sanbagawa belt, SW Japan. Journal of Structural Geology 17, 1077–1093.

Wallis, S.R., Platt, J.P., Knott, S.D., 1993. Recognition of syn-convergence extension in accretionary wedges with examples from the Calabrian Arc and the Eastern Alps. American Journal of Science 293, 463–494.